Thermochimica Acta, 229 (1993) 1–14
Elsevier Science Publishers B.V., Amsterdam

The derivation of thermodynamic properties by DSC: free energy curves and phase stability [1]

M.J. Richardson

National Physical Laboratory, Teddington, Middlesex TW11 0LW (UK)

(Received and accepted 1 June 1993)

Abstract

The derivation of enthalpies, entropies and free energies of fusion and transition from DSC curves is discussed. Although the apparent location of a thermal event is much influenced by rate effects, isothermal enthalpy changes are readily obtained by simple extrapolations. The corresponding entropies are always flawed by departures from reversibility and data must be corrected by forcing data to obey the condition that $\Delta G = 0$ at a first-order transition. Free energy curves may then be used to define the relative stabilities of different structures. Procedures are illustrated by examples from a series of liquid crystal-forming materials that show widespread solid-state polymorphism.

INTRODUCTION

Differential scanning calorimetry (DSC) has long had a quantitative potential which approaches that of the more traditional, but less versatile, adiabatic calorimetry. This potential should be increasingly exploited as digital data storage and computerised evaluation become ever more widely used. Unfortunately, there is a real danger that, instead, many of the procedures that were used to manipulate traces from chart recorders—and were, at best, only semi-quantitative—may simply be transferred to programmed forms: the net result will only be the more rapid production of incorrect data. The enthalpies of fusion or transition from phase x to phase y ΔH_{xy} (subscripts x,y may indicate c (crystal; c1, c2, etc. represent different structures), sA (smectic A), n (nematic), i (isotropic liquid)), that have long been reported are, in reality, very often complex functions of ΔH_{xy} and of Δc_{pxy}, the specific heat capacity difference $(c_{py} - c_{px})$ in the transition region. The corresponding entropy changes are similarly flawed and here there is the additional problem that the thermodynamic requirement for reversibility is not satisfied.

The aim of this paper is to show how thermodynamic properties can be

[1] Presented at the Tenth Ulm Conference, Ulm, Germany, 17–19 March 1993.

obtained from conventional DSC heat capacity measurements [1,2] without recourse to time-consuming extrapolations to zero heating rate. Special attention is given to the behaviour at phase changes with the final aim of defining the thermodynamic stability of a phase by the construction of free energy curves. The methods are illustrated by examples from a series of liquid crystal-forming materials that show widespread solid-state polymorphism. DSC is expecially useful in this context because, by using the rapid cooling and heating rates available in modern instruments, relatively unstable polymorphs (which would, for example, transform on the time scale required for conventional X-ray exposure) can be examined as a matter of routine.

EXPERIMENTAL

Materials

The methods discussed in this paper are illustrated by measurements on 4,4′-*n*-propoxy cyano-biphenyl and 4,4′-*n*-heptyl cyano-biphenyl, abbreviated to 3.OCB and 7.CB, respectively. These are M9 and K21 of Merck Ltd., Poole, England, from whom they were obtained. They were used as received: 3.OCB as solution-grown crystals and 7.CB as a supercooled nematic liquid.

Calorimetry

"Heat capacity" curves were obtained using differential scanning calorimetry (Perkin-Elmer DSC2) and procedures that have already been described [3]. The associated Intracooler unit gave a convenient minimum working temperature of 220 K. Samples were contained in sealed pans. Heating and cooling rates were generally 10 K min $^{-1}$.

Temperatures were corrected using an isothermal calibration plus an additional term for thermal lag that was determined from individual DSC curves [4]. The several transition temperatures that are given were determined by the step-wise isothermal procedure, except for the melting temperature of the solid phase 2 of 3.OCB. This was metastable near T_{c2i} and slowly transformed to the more stable state (see below). T_{c2i} was therefore obtained by noting the displacement of the two melting curves (Fig. 1) and subtracting this from T_{c1i}. That this procedure was fully justified is shown by the data for 7.CB; $T_{c1n} = 291.5$ K, $T_{c2n} = 303.3$ K, observed curve displacement = 12.0 K.

RESULTS

The melting curve of the original solution-grown crystals (c1) of 3.OCB is given in Fig. 1. Subsequent cooling showed the monotropic transition to the nematic phase at 337.7 K (X, Fig. 1) which only just preceded a crystallisation process that was apparently complete by about 327 K. There was, however, a final, rather sluggish, event that peaked around 308 K. The temperature range from 220 to 290 K gave an almost linear c_p–T curve that was the same in both cooling and subsequent heating. Melting of the DSC-crystallised material (c2) occurred at 344.0 K, 3.5 K below c1 (347.5 K). That this was not due simply to improved thermal contact after melting was shown by the reappearance of c1 on annealing just below 344 K. It will be seen later that the two forms also have different heats of fusion.

If cooling was stopped at 327–330 K and the sample reheated, it behaved very much like a simple mixture of c2 and isotropic liquid (69/31 by mass) although the two-stage nature of the crystallisation process shown in Fig. 1 implies that an intermediate structure was formed; if this is so, the thermal properties must be very similar to those of c2.

The behaviour of 7.CB was even more complex. The initial nematic phase could be supercooled to 270 K before the onset of crystallisation (Fig. 2, curve i). Reheating from 220 K gave two exothermic processes prior to melting at 303.3 K. Although the location and magnitude of the exotherms

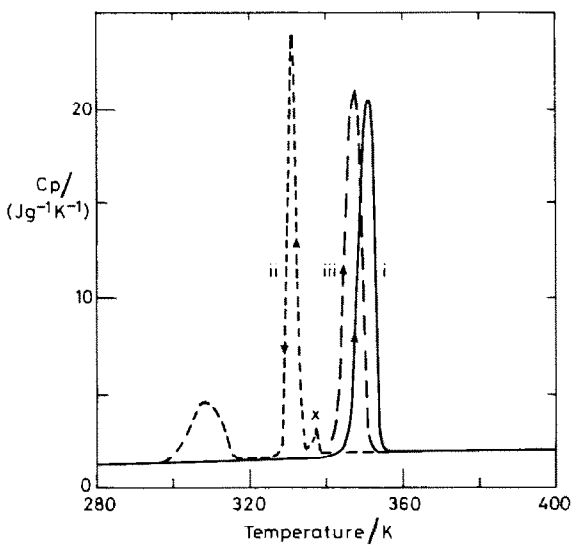

Fig. 1. Melting and crystallisation of 3.OCB. Numbers identify the systems on subsequent graphs. The isotropic → nematic transition is shown at X. Arrows indicate heating or cooling at 10 K min^{-1}.

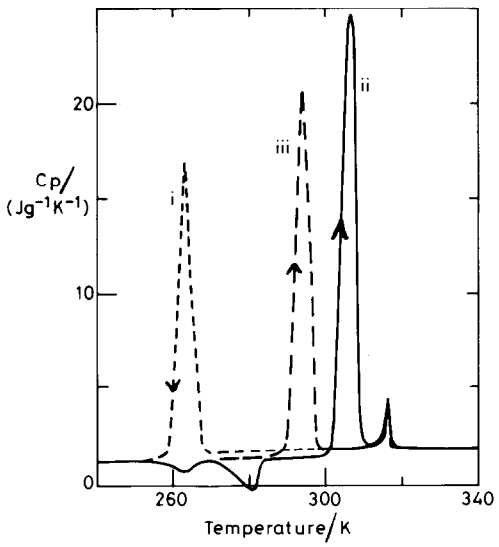

Fig. 2. Crystallisation and melting of 7.CB. The nematic ⇌ isotropic transition is completely reversible. Rates all $\pm 10\ \mathrm{K\ min^{-1}}$.

varied slightly from run to run, the melting process itself was very reproducible. If, however, the sample was isothermally crystallised at 270 K and then reheated (an additional isothermal "hold" at this temperature, from minutes to hours, had no further effect), both the melting point (291.4 K) and heat of fusion were reduced (Fig. 2, curve iii). The structure (c2), although melting nearly 12 K below that of c1, showed no tendency to revert to the latter and, if never cooled below 270 K, could be formed by various time/temperature programmes, always giving the same thermal properties. (There were indications that a third structure, $T_{c3n} = 296.2$ K, could be formed by a quench to 265 K followed by isothermal crystallisation, but growth conditions could not be varied sufficiently to eliminate the possibility of this being a heavily defected form of c1.) Any exposure to temperatures lower than 265 K invariably gave exotherms on reheating; the final form (c1) was stable to recycling in the range 220–300 K. Figure 3 shows, on an expanded scale, the crystallisation and melting of 7.CB over the range 340 ⇌ 240 K. Cooling was particularly helpful in this case because supercooling allowed a more complete definition of the behaviour of nematic phase: in heating, only a portion of the n–i transition was visible whereas cooling gave the whole transition plus, at lower temperatures, a simple linear c_{pn}–T region. It will be seen later that this last leads to an unambiguous determination of $\Delta H_{ni}(T)$ and, through this, $\Delta H_{cn}(T)$.

In the following discussion, data were only accepted if certain simple tests for thermodynamic consistency were valid.

(i) In stable regions (where no annealing or other anomalous behaviour was detectable on the time scale of the DSC experiment), c_p was the same

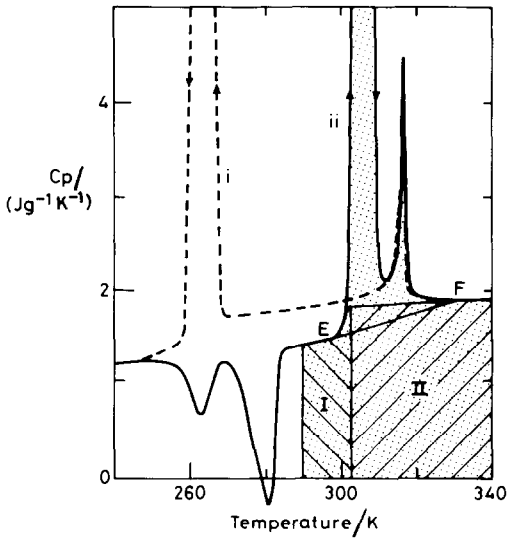

Fig. 3. Expanded section of Fig. 2 showing how the quantities of eqn. (1) and (1a) are defined for $T_1 = 290$, $T = 303.3$, $T_2 = 340$ K. Area Q is shaded.

(within experimental error) whether determined in heating or cooling modes. In Fig. 3, for example, $c_{pc2}(240\ \mathrm{K}) = 1.224(-)/1.212(+)\ \mathrm{J^{-1}\,g^{-1}\,K^{-1}}$; and $c_{pi}(340\ \mathrm{K}) = 1.913(-)/1.910(+)\ \mathrm{J\,g^{-1}\,K^{-1}}$, where (−)/(+) represent data obtained in cooling and heating, respectively.

(ii) The overall enthalpy change for the cycle: liquid(T_R) → solid A(T_1) → solid B(T_2) → · · · → liquid(T_R) should be zero. In Fig. 4,

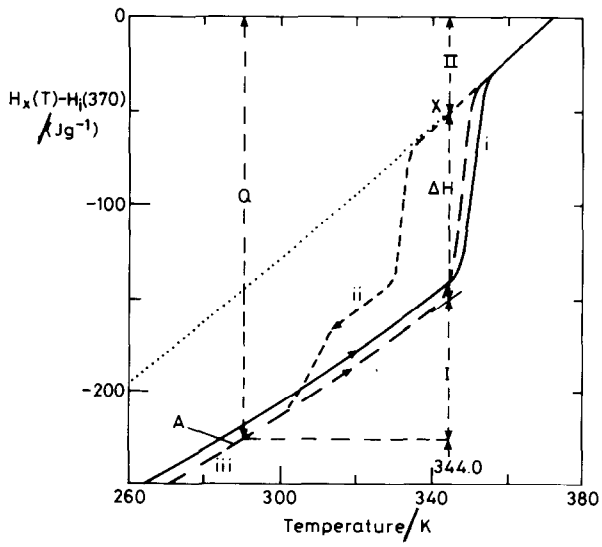

Fig. 4. Enthalpy changes for 3.OCB with respect to $H_i(370\ \mathrm{K}) \equiv 0$.

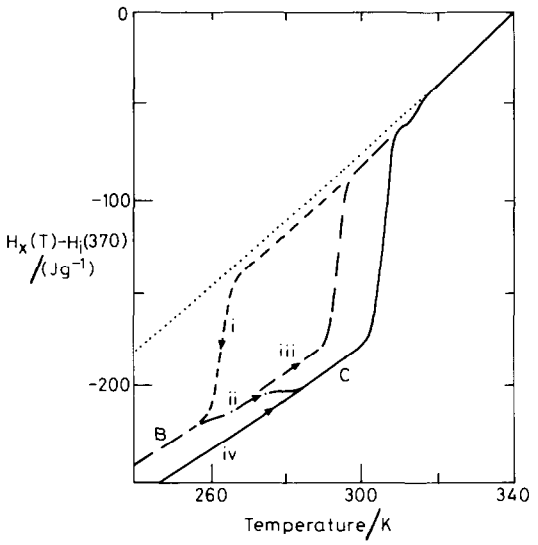

Fig. 5. Enthalpy changes for 7.CB with respect to $H_i(340\ K) \equiv 0$. Curve (iv) is not shown on Fig. 1; it refers to material, as in (ii), that has been annealed at 300 K before cooling and rerunning.

$H(370\ K) - H(290\ K) = 226.5(-)/227.2(+)\ J\ g^{-1}$, and in Fig. 5, $H(340\ K) - H(240\ K) = 240.9(-)/241.7(+)\ J\ g^{-1}$.

ENTHALPY CURVES: ENTHALPY OF FUSION OR TRANSITION

General

The "specific heat" curves of Figs. 1–3 are actually composites that include contributions from both c_p and ΔH_{xy}. A DSC-derived c_p–T curve is normally accurate to ±1% (as judged by comparison with results on materials with known c_p). This figure must, however, be qualified in the vicinity of most phase changes. In a DSC, melting of even an ultrapure metal appears to cover several degrees when in reality it requires less than 0.1 K, as may be shown by stepwise heating experiments. The apparent broad melting range is an artefact which reflects the time required to supply the massive (relative to c_p) heat of fusion to the sample. However, even though the *distribution* of enthalpy with temperature in a transition region is in error, the *overall change* remains correct to ±1% and suitable data treatment will give a truly thermodynamic enthalpy of transition. (It will be seen later than the situation is very different when entropy changes are considered.)

Enthalpy changes

The overall enthalpy change $H_y(T_2) - H_x(T_1)$ ($\equiv Q$) associated with the temperature interval from T_1 to T_2 (there is a phase change in this interval if $x \neq y$) is obtained by integration of the $c_p - T$ curve (the "baseline" here is effectively defined by the line $c_p = 0$).

For 3.OCB, the isotropic liquid heat capacity (c_{pi}) is a linear function of temperature over the range from 360 to 410 K. In Fig. 4, enthalpy changes, relative to $H_i(370\,K) = 0$, are plotted for the curves of Fig. 1 together with calculated values (using c_{pi}) for the supercooled liquid. The closure of the enthalpy cycle (curves (ii), including the i–n transition at X, and (iii)) is obvious together with the higher enthalpy of the original crystals (curve (i)). The *apparent* displacement of both melting regions to temperatures above the relevant T_{ci} is also clear. Similar curves for 7.CB, relative to $H_i(340\,K) = 0$, are shown in Fig. 5. Curves (iii) and (iv) are very reproducible but, although the enthalpy cycle for (i) and (ii) again closes, there may be variations of 3–4 J g^{-1} in $H(T) - H(340\,K)$ in the thermally inert region ($T < 250\,K$) between successive cycles. These are reflected in the original $c_p - T$ curves by minor differences in the 308 K event in cooling and in the exothermic portions in heating.

Enthalpy of fusion or transition

The total enthalpy change across a transition is easily resolved into contributions from the isothermal enthalpy of transition and from specific heat terms. A general procedure is to extrapolate the low and high temperature c_p behaviour to a temperature T that is normally the relevant transition temperature T_{xy} but it may also be some common arbitrary value, for example when comparing data from a family of related materials. The relevant equations are

$$\Delta H_{xy}(T) = H_y(T) - H_x(T)$$
$$= [H_y(T_2) - H_x(T_1)] - [H_x(T) - H_x(T_1)] - [H_y(T_2) - H_y(T)] \quad (1)$$
$$= Q - I - II \quad (1a)$$

where Q, I and II refer to the three square-bracketed terms. The three quantities are shown in Fig. 4 for c2 and $T = 344.0$ K ($= T_{c2i}$) with $T_2 = 370$ K and $T_1 = 290\,K$. By using eqn. (1), the effects of premelting, the finite rate of temperature changes, and of postmelting (see below) are eliminated.

The heats of fusion or transition are shown in Figs. 6 and 7 for 3.OCB and 7.CB, respectively. In these, the dotted lines show idealised behaviour with no premelting and with all ΔH_{xy} taken in at T_{xy}. The effect of

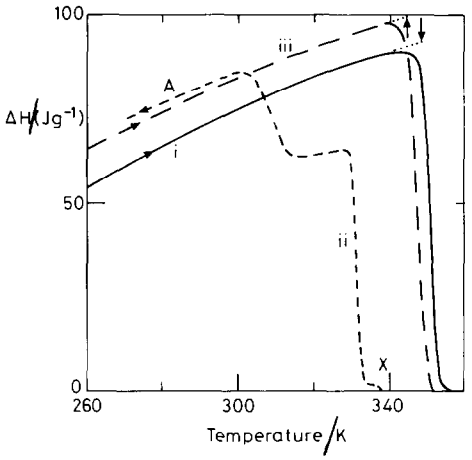

Fig. 6. The heat of fusion of 3.OCB. See text for discussion.

temperature on ΔH_{xy} is clearly shown by the great reduction in ΔH on crystallisation. Data at the respective transition temperatures are: 3.OCB, ΔH_{c1i}(347.5 K) = 92.3 J g^{-1}, ΔH_{c2i}(344.0 K) = 100.4 J g^{-1}; 7.CB, ΔH_{c1n} (303.3 K) = 96.7 J g^{-1}, ΔH_{c2n}(291.5 K) = 77.3 J g^{-1}, ΔH_{ni} = 7.1(291.5), 6.7(303.3), 5.9 J g^{-1}(316.0 K). Premelting, as judged by the departure from a linear c_{pc}–T relationship, reduces these by several percent and a comparison of normal, coarse-scale c_p–T curves (that is, those showing the complete peak) with expanded-scale curves shows that the former can conceal the onset of melting by several degrees. This probably accounts for some, at least, of the "linearising constant" needed to give straight lines in the standard DSC method of purity determinations [5].

The areas corresponding to *Q*, *I* and *II* (Fig. 3) define the correct

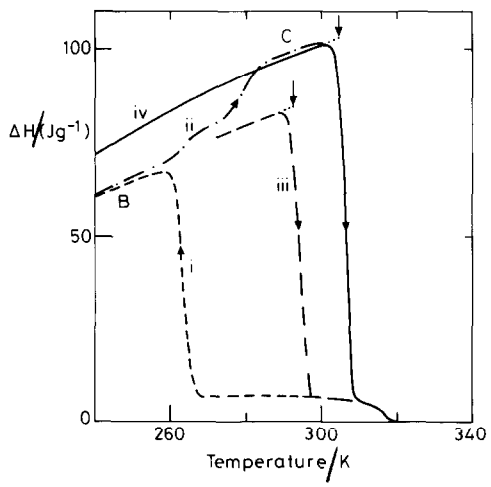

Fig. 7. The heat of fusion of 7.CB. See text for discussion.

(discontinuous) baseline that should be used for the determination of $\Delta H_{xy}(T_{xy})$ from a DSC curve. Current practice actually uses a single straight line (e.g. EF in Fig. 3) that hopefully approximates the correct construction: the resultant error in ΔH_{xy} depends very much on Δc_{pxy} and on the location of E and F (it can be positive or negative) but with modern data treatment there is no reason to introduce incorrect procedures that can invalidate the claimed limits of accuracy. When the c_p–T data of Figs. 1–3 are available, it is possible to relate "ΔH" obtained using a linear baseline to basic thermodynamic quantities: the "EF" construction gives the total enthalpy change from T_E to T_F less a contribution from the mean specific heat, i.e. $Q - 0.5[c_{py}(T_F) + c_{px}(T_E)]\ (T_F - T_E)$, where $T_2 = T_F$ and $T_1 = T_E$ and Q is as defined in eqns. (1) and (1a).

The procedures used here implicitly assume (through term II) that linear c_{pi}–T behaviour continues to low temperatures. Although there is no direct proof of this, indirect evidence from both CB and OCB homologues supports this view. In any case the point is only of academic interest for a given material, provided *consistent* c_{pi} data are used. In Figs. 6 and 7, for example, c_{pi} values from individual runs have been deliberately retained to give an indication of the effects of minor variations in c_{pi} which lead to inconsistencies in region A (Fig. 6), and B and C (Fig. 7). Reference to Figs. 4 and 5 shows that the enthalpy cycles are effectively closed in these region; the problems of Figs. 6 and 7 are caused by differences in extrapolated values of c_{pi}. When a common "least-squares" c_{pi}–T equation is used, the several curves again come into coincidence. Further discussion of the precautions needed for a proper definition of c_{pi} follows below. To use eqn. (1) effectively, the temperature range covered should be such that at T_1 and T_2, only normal c_p processes are active—premelting, annealing and similar phenomena must be absent, otherwise the "baseline" extrapolation to T_{xy} will be incorrect.

Baseline effects are especially important for low energy transitions such as those found for liquid crystals. For 7.CB, the supercooled nematic phase shown in Fig. 3 allows the direct application of eqn. (1) and the resulting ΔH–T curve is given in Fig. 8. It is clear that processes both below and, surprisingly, above T_{ni} ("postmelting") can falsify the apparent ΔH_{ni}, again in either direction. Sub-T_{ni} effects can perhaps be ascribed to changes in the ordering parameter δ, but the apparent residual "structure" above T_{ni} is less easy to explain. An anomalous c_{pi} region above either T_{ni} or T_{sAi}, with $dc_{pi}/dT \leqslant 0$, is found for all the CB and OCB homologues (from 1–12) examined and also for many other types of liquid crystals.

These effects are certainly not caused by instrumental artefacts: cooling and heating curves almost superimpose (Fig. 3) and the former always "anticipate" the approach to the liquid-crystalline state by the anomalous behaviour mentioned. The treatment according to eqn (1) integrates all the unusual enthalpy requirements and the extrapolated value of ΔH_{ni} at

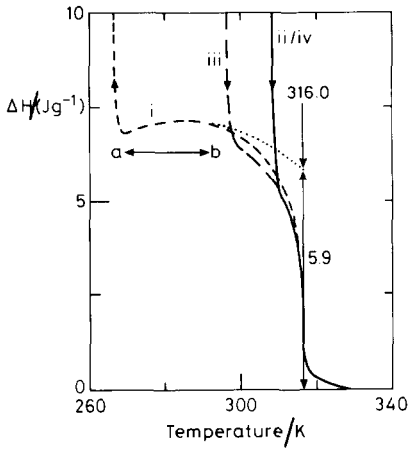

Fig. 8. The nematic region for 7.CB; c_{pn} is a linear function of temperature in the region ab, extrapolation to $T_{ni} = 316.0$ K is shown.

316.0 K (5.9 J g^{-1}) presumably refers to a limiting, low temperature δ value; anything else must be very heavily qualified to give it a valid meaning. Because of the anomalous "c_{pi}" region it was important to ensure that c_{pi} was representative of a truly isotropic liquid for the subsequent extrapolations (II in eqn. (1a)) to lower temperatures: samples were therefore always heated some 50–60 K above T_{ni} so that the appropriate c_{pi} region could be identified by at least 40 K of linear c_{pi}–T behaviour.

Multiple transitions

Equation (1) may be used to obtain any ΔH_{xy}, but when there are several transitions prior to the isotropic liquid it is often helpful to derive all ΔH in terms of $\Delta H_{xi}(T)$, $\Delta H_{yi}(T)$, etc. and to obtain $\Delta H_{xy}(T)$ by subtraction. This procedure was used for the two ΔH_{cn} values given earlier for 7.CB. This was possible because, as already discussed, the extensive supercooling of the nematic phase allowed an unambiguous determination of ΔH_{ni}. This is not always possible and in these circumstances the deconvolution of a multiple event becomes rather subjective: there is no way, for example, that the *heating* curves of Figs. 2 and 3 could define ΔH_{ni} with any accuracy, although this can only be fully appreciated by reference to Fig. 8. In a similar vein, ΔH_{ni} for 3.OCB can only be roughly estimated because of the proximity of crystallisation (X, Fig. 1). Sometimes, of course, it is essential to know $\Delta H_{xi}(T)$ even if several other transitions $x \rightarrow y \rightarrow z \rightarrow \cdots \rightarrow i$ intervene; for example, when correlating results for a homologous series with a common structure x. (The direct addition of individual enthalpies of transition can lead to gross errors because the differing specific heats of the several phases are neglected.)

ENTROPY AND FREE ENERGY CHANGES

The formal calculation of entropy changes $S_y(T_2) - S_x(T_1)$ ($\equiv S$) from c_p–T data requires the summation from T_1 to T_2 of terms of the form $c_p(T_v)\delta T_{uw}/T_v$ for successive values, $c_p(T_u)$, $c_p(T_v)$, $c_p(T_w)$, where $\delta T_{uw} = (T_w - T_u)/2$; δT_{uw} is a small temperature increment, of the order of a few tenths of a degree in this work. This is an acceptable procedure away from the transition regions when a correctly calibrated instrument gives a good approximation to equilibrium data. However, within such a region, as already discussed, there is an *apparent* displacement of heating curves to higher temperatures and this means that the entropy change calculated from the observed curve is less than the true value. The equivalent error in cooling experiments, when samples can often supercool many tens of degrees, will be even larger, and of opposite sign.

The problems of reversibility can be formally overcome by letting $S = S' + \delta S$ where S is the *reversible* quantity defined above, S' is the directed computed (or "observed") value and δS is the correction needed to restore reversibility. Entropic analogues of eqns. (1) and (1a) can then be written.

$$\Delta S_{xy}(T) = S_y(T) - S_x(T) = S - [S_x(T) - S_x(T_1)] - [S_y(T_2) - S_y(T)] \quad (2)$$

$$= S' + \delta S - III - IV \quad (2a)$$

where *III* and *IV* are abbreviations for the two square-bracketed terms of eqn. (2); they refer to idealised, reversible paths and may be calculated via c_{px} and c_{py}, respectively. At any transition temperature T_{xy}, the Gibbs free energies G of the two phases are equal, so that

$$\Delta G_{xy}(T_{xy}) = G_y(T_{xy}) - G_x(T_{xy}) = \Delta H_{xy}(T_{xy}) - T_{xy}\,\Delta S_{xy}(T_{xy}) = 0 \quad (3)$$

$$= Q - I - II - T_{xy}(S' + \delta S - III - IV) = 0 \quad (4)$$

δS can therefore be calculated from eqn. (4) at T_{xy}. Corrected, reversible, entropy changes are then converted to $\Delta S_{xy}(T)$ via eqn. (2a) and these, in turn, are used to derive $\Delta G_{xy}(T)$.

The several entropies and free energies are shown in Fig. 9 for the c1 form of 3.OCB. Full lines refer to "observed" values (S' only) and corrected, reversible data are shown as dashed lines.

Corrections to ΔS are about 1–2% and it is useful to note their magnitude and sign as a check on the consistency of the results: sample size, heating/cooling rate and even the type of pan (the larger basal area of conventional pans leads to a slight reduction in $|\delta S|$). It is because of this ability to monitor the behaviour of δS that the two terms S' and δS are not combined into a single unknown. An equivalent procedure is to *assume* a reversible path (no pre-/postmelting, all ΔH taken in at T_{xy}) and calculate entropy changes appropriately. *Some* premelting is truly reversible and in

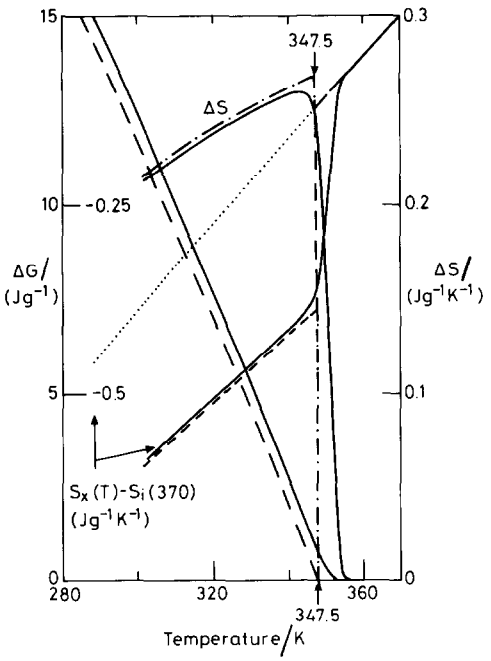

Fig. 9. Entropies and free energies for 3.OCB derived from curve (i) of Fig. 1: full lines, before correction for irreversibility; dashed lines, after correction.

this sense the procedure outlined overcompensates for irreversibility, but the effect is minor and the practical consequences are negligible.

When a sample shows multiple transitions, it is convenient to refer all to a common reference state, generally the isotropic liquid, and, provided that T_{xy} is known, a succession of corrections for kinetic effects at the various T_{xy} can be made. If, for example, a material undergoes transitions, $. \rightarrow \beta \rightarrow \alpha \rightarrow i$, then the initial correction $\delta S_{\alpha i}$ allows the calculation (eqn. (4)) of $\Delta G_{\alpha i}$ at $T_{\beta\alpha}$, and this is equated with $\Delta G_{\beta i}$ at $T_{\beta\alpha}$ to obtain $\delta S_{\beta\alpha}$, the same procedure as in eqns. (3) and (4) above but with a non-zero value of ΔG. In this way a family of free energy curves can be built up relative to some reference state at the same temperature: curves are always ΔG rather than G.

Free energy curves relative to the isotropic liquid, $\Delta G_{xi}(T)$, are shown in Fig. 10 for 3.OCB and 7.CB. Curves for the former intersect at 310 K showing how the stability (the phase with the *maximum* ΔG_{xi}, equivalent to the minimum G_x) changes with temperature. It is naturally tempting to assume that the highest-melting phase is also the most stable at room temperature but this is not the case for 3.OCB. Here free energy curves cross because of the large difference in ΔH for the two solid phases; the location of the crossover can only be found by using the thermodynamic procedures outlined here. Of course, thermodynamics alone gives no

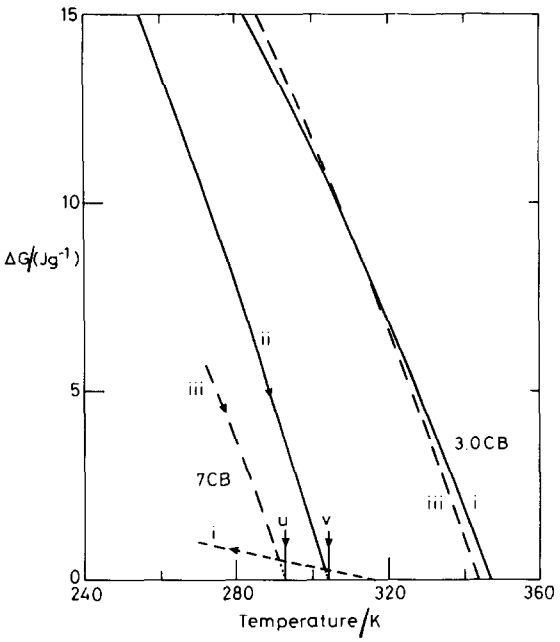

Fig. 10. Free energies relative to the isotropic liquid at the same temperature, for the structures of Figs. 1 and 2. Extrapolated melting points (see text) are indicated at u and v.

information concerning the rate of transition from c1 → c2 at room temperature, but if stability is critical, as with a drug, for example, it is obviously unwise to assume that no change will take place on storage. The ΔG curves for 7.CB show that the lower melting form is always metastable over the temperature range considered. For both structures, it is a simple matter to calculate the "melting points' and associated $\Delta H_{xi}(T_{xi})$ that would be found if the nematic phase did not intervene. This, again, may allow a more meaningful comparison of data for the homologues: for both CB and OCB systems, some members melt directly to the isotropic liquid, others go via nematic and/or smectic A phases; without T_{xi} and related data, it is difficult to correlate changes in properties with chain length, for example.

CONCLUSIONS

Although DSC has long had the potential for thermodynamic measurements, this has rarely been exploited. Quantitative work is not difficult but the treatment of data requires numerous tedious operations that were impractical in the age of chart recorders but are ideally suited to modern microprocessors. Unfortunately, few manufacturers supply appropriate software and, as a result, most DSC-based "thermal properties" can be faulted in some way. This is unfortunate because much current instrumentation will give c_p to ±1% and it is possible to construct a sound

thermodynamic structure on this foundation. The development of such a structure and its application in studies of phase stability have been described here. Subsequent papers will discuss the polymorphic behaviour of the CB and OCB homologoues.

REFERENCES

1 M.J. Richardson and N.G. Savill, Thermochim. Acta, 30 (1979) 327.
2 G.W.H. Höhne, Thermochim. Acta, 187 (1991) 283.
3 M.J. Richardson, in K.D. Maglic, A. Cezairliyan and V.E. Peletsky (Eds.), Compendium of Thermophysical Property Measurement Methods, Vol. 2, Plenum, New York, 1992, p. 519.
4 M.J. Richardson and N.G. Savill, Thermochim. Acta, 12 (1975) 213.
5 Z.-W. An and R. Sabbah, Thermochim. Acta, 190 (1991) 241.